

Bunched fluxon states in one-dimensional Josephson-junction arrays

Alexey V. Ustinov

Physikalisches Institut III, Universität Erlangen-Nürnberg, D-91058 Erlangen, Germany

Boris A. Malomed

Department of Interdisciplinary Studies, Faculty of Engineering, Tel Aviv University, Tel Aviv 69978, Israel

Shigeki Sakai

Electrotechnical Laboratory, 1-1-4 Umezono, Tsukuba-shi, Ibaraki 305, Japan

(Received 1 October 1997)

Dynamics of fluxons in a discrete Josephson transmission line is investigated, combining numerical simulations and an analytical approach. It is found that, in different ranges of the parameters (the driving dc bias current and dissipative constant), two fluxons (2π -kinks) may form either a bifluxon (4π -kink), or various bound states ($2\pi+2\pi$ -kinks with a finite separation), which can stably propagate along the line. The stability of these states is investigated as a function of the kink velocity. An analytical approach is based on prediction of formation of a two-kink bound state through the interaction mediated by their oscillating "tails." At small velocities, a satisfactory agreement is found between the analysis and the numerical results. At still smaller velocities, a new phenomenon is predicted analytically and found numerically, viz., transition from an asymmetric "tailed" kink to a symmetric tailless one. Conditions for experimental observation of the predicted behavior, as well as its practical consequences for the fluxon propagation in the discrete Josephson transmission lines, are discussed too. [S0163-1829(98)10417-4]

I. INTRODUCTION

Parallel-coupled one-dimensional Josephson junction arrays, also known as discrete Josephson transmission lines (DJTLs), have received a considerable interest over the last years.^{1,2} Such an array is described by the discrete sine-Gordon equation (DSGE) and represents an experimental realization of the driven underdamped one-dimensional sine-Gordon (SG) lattice, which finds applications in many other fields of physics.³ A ballistic 2π -kink in the discrete SG lattice corresponds to a Josephson vortex, or fluxon, which can propagate in a DJTL. DSGE is much simpler for numerical studies than the continuum SG equation, and its first numerical and experimental investigations have been initiated long ago.⁴ However, due to the nonintegrability of the DSGE, very limited progress in analytical approaches has been reported thus far. Recently, an earlier prediction of resonances between moving fluxon and its radiation in a DJTL (Ref. 1) has been confirmed experimentally.² A number of experiments⁵⁻⁷ and theoretical approaches⁸ were reported lately.

Peyrard and Kruskal⁹ were first to point out that, even for large discreteness, a localized kink in the SG lattice may exhibit some solitonic features close to those in the continuum SG solitons. In the same work, it had been shown numerically that, in the absence of losses and at a sufficiently high velocity of the kink, the strongly discrete SG model permits stable propagation of strongly localized multi- 2π -kinks (i.e., 4π -kinks, 6π -kinks, etc.). Until now, the multi- 2π -kinks in real physical systems have not been observed experimentally. It is therefore relevant to search for such higher-order kink solutions numerically in an experimentally realistic parameter range of a DJTL, using the per-

turbed DSGE with the friction and driving forces. If they exist, the multi- 2π -kinks might be relevant for applications of DJTL to superconducting electronics.

In this work, we investigate dynamics of fluxons in DJTLs numerically and, partly, also analytically. In order to separate new effects from the previously known fluxon-radiation resonances,^{1,2} we consider a very long system with periodic boundary conditions, i.e., a long annular DJTL. In Sec. II we show numerically that, depending on the initial location, a pair of fluxons (2π -kinks) may form either a bifluxon (4π -kink) with no separation between the constituent fluxons, or a hierarchy of their bunched states [$(2\pi+2\pi)$ -kinks] that can propagate along the DJTL, keeping a constant separation between the bound fluxons. Stability of these states is investigated as a function of the driving force and fluxon's velocity. Conditions for experimental observation of the predicted behavior, as well as some practical consequences for the propagation of fluxon pulses in discrete Josephson transmission lines, are also discussed. The analytical approach to the description of the bunched states (presented in Sec. IV) will be based on consideration of interactions between the two 2π -kinks mediated by their "tails." An essential peculiarity of the present problem is that the two tails of a moving kink (the front tail and the trailing one) are strongly different. The bunched state is possible when the trailing tail is oscillating. Analyzing the tail structure, in Sec. III we will find analytically and will then check numerically that there is a critical value of the velocity below which the oscillating tails disappears, which implies existence of a dynamical phase transition in DJTL, namely, a transition between the "dimer" (or "polymer") states and a gas of free fluxons in a sufficiently long DJTL.

To conclude the introduction, it is relevant to stress that

the bunched states are also possible in the continuum long Josephson junction, but only if one takes into account, besides the usual dissipative term, the so-called surface losses, that give rise to an extra diffusion term in the corresponding SG equation. Due to the presence of this term, the fluxons moving with a sufficiently large velocity can develop an oscillating tail, that gives rise to a bunched state. This fact was first discovered in computer simulations many years ago.¹⁰ It has also been demonstrated numerically¹¹ that fluxons moving at a velocity close to the Swihart velocity indeed possess a trailing oscillating tail. The first experimental indication to bunching of the fluxons in the long Josephson junction through this mechanism has been found by measuring the emitted radiation in a linear junction.¹² The analytical approach to the formation of the bunched states in the driven damped SG model was developed in detail in Ref. 13. In the discrete SG model, in contrast to the continuum one, the bunched states may exist even without any dissipation.

II. SIMULATIONS OF THE BUNCHED STATES OF THE FLUXONS

The discrete Josephson transmission line is described by the discrete version of the perturbed SG model

$$\frac{d^2\phi_n}{dt^2} + \alpha \frac{d\phi_n}{dt} + \sin\phi_n + \gamma - \frac{1}{a^2}(\phi_{n-1} - 2\phi_n + \phi_{n+1}) = 0, \quad (1)$$

where the individual junction's number, n , takes values $0 \leq n \leq N$, ϕ_n is the superconducting phase difference on the n th junction, and a is the normalized spacing of the discrete line which is often also called discreteness parameter. To simplify comparison with the continuum case, all the parameters in Eq. (1) are written in the standard notation similar to that used in the continuum SG model: the spatial coordinate x is normalized to the effective Josephson penetration depth, the time t is normalized to the inverse plasma frequency $\omega_0^{-1} = [\Phi_0 C / J_c]^2$, C is the mean capacitance per unit length of the array, α is a dissipation coefficient, and γ is the bias current per unit length normalized to the spatially averaged critical current density $J_c = I_c / D$, I_c and D being the critical current of an isolated junction and the distance between the neighboring junctions in physical units. Equation (1) is written in the simplest approximation neglecting all mutual inductances between different cells in the array. A complete model of DJTL, including long-range mutual inductances, has been considered in Ref. 14. In relation to the above mentioned surface losses in long continuous junctions, we note that the corresponding term is neglected in Eq. (1).

In order to study interactions between moving fluxons in the most clear form, we simulated Eqs. (1) with periodic boundary conditions, identifying the points $n=0$ and $n=N$ in Eqs. (1) and assuming $\phi_N = \phi_0 + 2\pi N_{\Phi}$, where N_{Φ} is the number of the fluxons trapped in the ring array. In the simulations presented in this work, we considered the simplest cases with one or two trapped fluxons. The integration was performed using the fourth-order Runge-Kutta scheme with the time step $\Delta t = 0.025$.¹

The numerically found kink (fluxon) solution to Eq. (1) is shown in Fig. 1. Displayed is an instantaneous profile of the

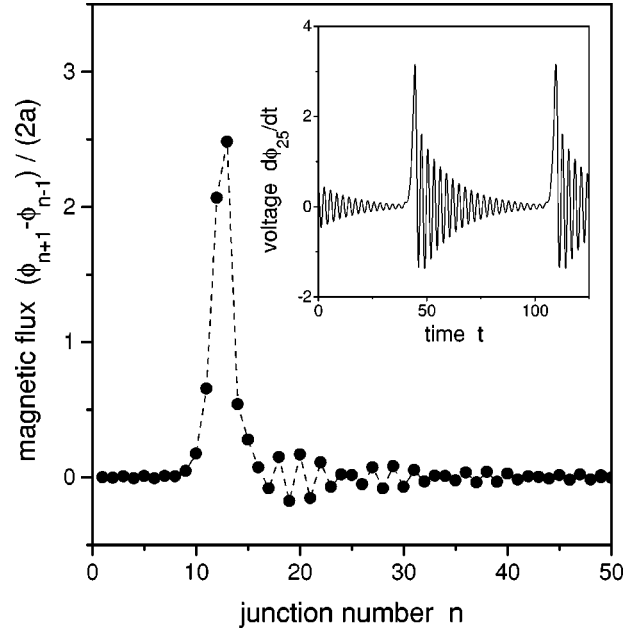


FIG. 1. Numerically calculated instantaneous profile of the local magnetic flux as a function of the cell number corresponding to a single fluxon propagating through a one-dimensional annular Josephson junction array (from the right to the left). The parameters used are the normalized array length $L = 50$, the discreteness parameter $a = 1.0$, the dissipation coefficient $\alpha = 0.1$, and the bias current $\gamma = 0.4$. The inset shows the time evolution of the voltage at the junction with the number $n = 25$.

magnetic flux per cell as a function of the junction number n , that corresponds to a single fluxon propagating from the right to the left. Starting from the initial configuration in the form of the 2π -kink solution to the continuum SG equation, $\phi_n = 4 \arctg[\exp(an + vt - x_0 / \sqrt{1 - v^2})]$ (where the continuum coordinate x is substituted by the discretely varying distance an) with the velocity $v = 0.9$ and $x_0 = 20$, Eq. (1) has been integrated over 500 time units. The steadily moving fluxon with a well-established velocity $v_{1F} \approx 0.768$ has been obtained. The inset shows evolution of the local voltage $d\phi_n(t)/dt$ at the individual junction with the number $n = 25$. One clearly sees the oscillating “tail,” i.e., decaying oscillations in the wake of the passing kink. These oscillations are due to the discreteness of the transmission line and are discussed in more detail in the next section.

In order to trigger a bifluxon in our numerical experiment, the simulations were started from the initial conditions corresponding to two identical continuum SG 2π -kinks placed at the same position $x = 0$ and moving initially at the velocity $v = 0.9$. After a transient period, a steady state is reached in the form of a localized single 4π -kink propagating at the velocity $v_{2F} \approx 0.853$. The local voltage evolution for this state is shown in Fig. 2(a), with the other parameters being the same as for Fig. 1. We note that at the same bias current γ the established velocity v_{2F} of the two-fluxon 4π -kink is larger than that of the single-fluxon 2π -kink v_{1F} . Three plots in Fig. 2 show a change in the local voltage evolution at the individual junction with the number $n = 25$ as the bias current γ is decreased from $\gamma = 0.40$ (a) to $\gamma = 0.15$ (c). We find that, with decrease of the bias current, the velocity of the fluxons is decreasing and the 4π -kink transforms into a

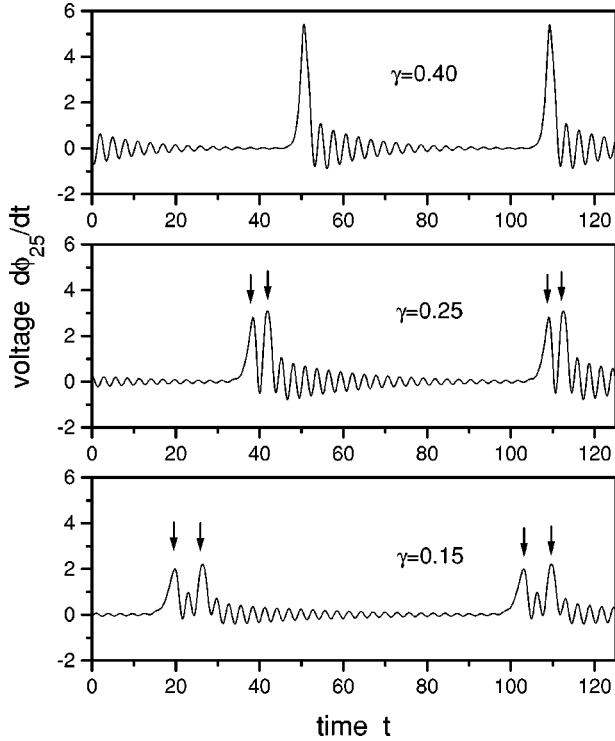


FIG. 2. Bifluxon propagating in the one-dimensional annular Josephson junction array with $L=50$, $a=1.0$, and $\alpha=0.1$. Three plots show the time evolution of the voltage at the junction with $n=25$ at $\gamma=0.40$ (a), $\gamma=0.25$ (b), and $\gamma=0.15$ (c), respectively.

pair of separated but closely bound 2π -kinks, which are marked by the arrows in Figs. 2(b) and 2(c). At a fixed bias current γ , the spacing between the kinks remain constant for arbitrary long integration time (time intervals up to $t=10000$ have been tested). One can notice that the bunched states of two 2π -kinks in Figs. 2(b) and 2(c) differ from each other by the number of the oscillations trapped between the two bunched kinks passing the observation point.

As a general characteristic of the $(2\pi+2\pi)$ -kinks (bunched states), showing their dependence upon the driving force (bias current), we have simulated the current-voltage characteristics (IVC) of the DJTL. The voltage is proportional to the mean velocity of the moving kink(s), that is determined by the balance between the driving force $\sim \gamma$ and the friction force generated by the viscosity α and radiation losses. Figure 3 shows the full IVC for various $(2\pi+2\pi)$ -kink bunched states in the long array with $L=100$, $a=1.0$, and $\alpha=0.1$. The voltage axis actually shows the kink's velocity v normalized to the maximum propagation velocity of the linear electromagnetic waves in the continuum system (the Swihart velocity). The arrows indicate branches corresponding to the different bunched states: (A) the 4π -kink [see Fig. 2(a)]; (B) the first $(2\pi+2\pi)$ -kink bunched state [see Fig. 2(b)]; (C) the second $(2\pi+2\pi)$ -kink bunched state (see Fig. 2c); (D) the third $(2\pi+2\pi)$ -kink bunched state. IVC was calculated starting from $\gamma=0.5$ with the initial conditions taken as a juxtaposition of two continuum sG 2π -kinks moving at the velocity $v=0.9$. After finding a steady state, the bias current γ was varied by small steps of $\Delta\gamma=0.005$, in order to move along the IVC. With the increasing bias, at $\gamma\approx 0.63$, the system

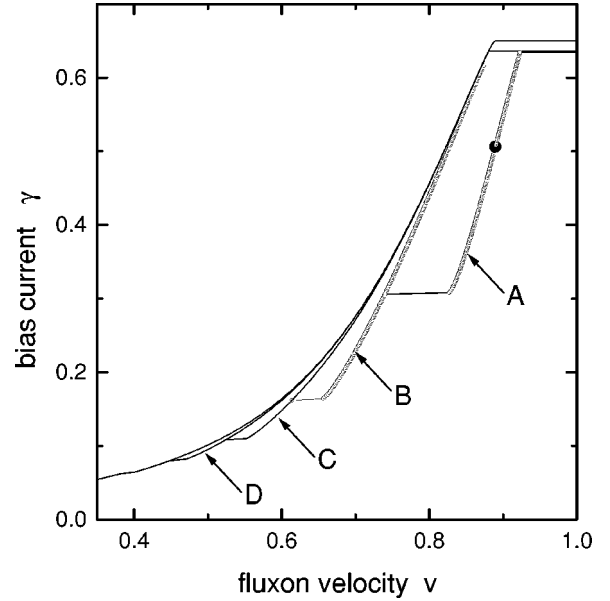


FIG. 3. Calculated two-fluxon current-voltage (v vs. γ) characteristics for the one-dimensional annular Josephson junction array with $L=100$, $a=1.0$, and $\alpha=0.1$. The voltage axis shows the normalized fluxon velocity v . The arrows indicate branches corresponding to different fluxon bunched states: (A) the 4π -kink; (B) the first $(2\pi+2\pi)$ bunched state; (C) the second $(2\pi+2\pi)$ bunched state; (D) the third $(2\pi+2\pi)$ bunched state.

switched into a high-voltage state corresponding to a quickly whirling background. With decrease of γ from the initial point $\gamma=0.5$, we have found a sequence of switchings between the different bunched states: $A \rightarrow B \rightarrow C \rightarrow D \rightarrow \dots$. For any of these states, further increase of the bias revealed a hysteresis which is clearly seen in Fig. 3.

Thus, the most salient feature of Fig. 3 is that, with the decrease of the driving force, the 4π -kink turns into the first bunched $(2\pi+2\pi)$ -kink state at a certain velocity $v=v_{\min}^{(0)}$, the latter state then jumps into the next one at $v=v_{\min}^{(1)}$, and so on. A challenging problem for analytical consideration is to evaluate the critical velocities $v=v_{\min}^{(k)}$ with $k=0,1,2,\dots$, at which the transitions between different branches of IVC occur. This will be a subject of the next sections.

III. THE ANALYTICAL APPROACH: A SINGLE KINK

The basic part of the analytical approach is consideration of the ‘‘tails’’ of the kink solution described by the linearized equation (1). Substituting into this equation $\phi_n = -\sin^{-1}\gamma + \psi_n$ and linearizing it with respect to small ψ_n , we obtain

$$\frac{d^2\psi_n}{dt^2} + \alpha \frac{d\psi_n}{dt} - \frac{1}{a^2}(\psi_{n-1} + \psi_{n+1}) + \left(\frac{2}{a^2} + \sqrt{1-\gamma^2} \right) \psi_n = 0. \quad (2)$$

Assuming γ small, we will replace in this equation $\sqrt{1-\gamma^2}$ by 1.

A solution to Eq. (2) is looked for in the form

$$\psi_n = e^{-p(n-vt)}, \quad (3)$$

where p is a (generally, complex) wavenumber. Substitution of Eq. (3) into Eq. (2) yields

$$p^2 v^2 + \alpha p v - \frac{2}{a^2} \cosh p + \frac{2}{a^2} + 1 = 0. \quad (4)$$

Because p is complex, we substitute into Eq. (3) $p = p_r + i p_i$, with the intention to split it into two real equations for p_r and p_i :

$$(p_r^2 - p_i^2) v^2 + \alpha v p_r - \frac{2}{a^2} \cosh p_r \cos p_i + \frac{2}{a^2} + 1 = 0, \quad (5)$$

$$p_r p_i v^2 + \frac{1}{2} \alpha v p_i - \frac{1}{a^2} \sinh p_r \sin p_i = 0. \quad (6)$$

In a sufficiently long system, one has an exponentially decaying tail with no oscillations in front of the moving kink (region I), which corresponds to the solution (3) with $p_r^I > 0$ and $p_i^I = 0$, the superscript referring to the region I. As it follows from Eq. (5), the value of p_r^I is determined by the simplified equation, in which in the zeroth-order approximation we will also set $\alpha = 0$:

$$(p_r^I)^2 v^2 - \frac{4}{a^2} \sinh^2 \left(\frac{1}{2} p_r^I \right) + 1 = 0. \quad (7)$$

Behind the kink (region II), one should have a trailing oscillating tail corresponding to the solution (3) with $p_r^{II} \leq 0$ and $p_i^{II} \neq 0$. However, the condition $p_r^{II} \leq 0$ is *not* satisfied automatically, hence it imposes a nontrivial limitation on a parametric region in which the kink with the oscillatory trailing tail, capable to give rise to the bunched states, can exist in the damped discrete system. Because Eqs. (5) and (6) are quite complicated in the general case, we will consider this issue in detail in the analytically tractable and experimentally important limit, when the dissipative constant α is small. In the zeroth-order approximation, one obtains an equation for p_i^{II} by setting $p_r^{II} = 0$ and $\alpha = 0$ in Eq. (5):

$$(p_i^{II})^2 v^2 - \frac{4}{a^2} \sin^2 \left(\frac{1}{2} p_i^{II} \right) - 1 = 0. \quad (8)$$

Still, this equation cannot be solved analytically. However, one can immediately solve it for the kink's velocity, regarding it as a function of p_i^{II} :

$$v^2 = (p_i^{II})^{-2} \left[\frac{4}{a^2} \sin^2 \left(\frac{1}{2} p_i^{II} \right) + 1 \right]. \quad (9)$$

Moreover, as the parameter p_i^{II} is large for small velocities, one may replace the rapidly oscillating expression $\sin^2(\frac{1}{2} p_i^{II})$ by its mean value $\frac{1}{2}$. Then, one immediately obtains an approximate solution

$$p_i^{II} \approx \sqrt{2 + a^2 / \alpha v}. \quad (10)$$

It is relevant to mention that, in order to proceed to the continuum limit, one should set $p \equiv a \tilde{p}$ and $v \equiv a^{-1} \tilde{v}$, where \tilde{p} and \tilde{v} will be the wave number and velocity in the continuum limit, and then set $a \rightarrow 0$. In this limit, Eq. (9) reduces to $\tilde{v}^2 = 1 + \tilde{p}^{-2}$. However, a well-known fact is that no stable kink with the velocity $\tilde{v}^2 > 1$ is possible in the continuum SG equation. Thus, a stable kink with the oscillating trailing tail may exist *only* if the system is sufficiently far from the continuum limit. (In the continuum model, the oscillating tail can be generated only by the above-mentioned surface loss term as discussed in the Introduction.)

To calculate a small real part of the wave number in the next approximation with respect to the small dissipative constant α , one should linearize Eq. (6) with respect to p_r^{II} and α , which yields

$$p_r^{II} = - \frac{\alpha v}{2} \left(v^2 - \frac{\sin p_i^{II}}{a^2 p_i^{II}} \right)^{-1}. \quad (11)$$

Finally, inserting Eq. (9) into (11), we obtain the necessary condition $p_r^{II} \leq 0$ for existence of the oscillating tail in the form

$$a^2 > p_i^{II} \sin p_i^{II} - 4 \sin^2 \left(\frac{1}{2} p_i^{II} \right). \quad (12)$$

Notice that, at $0 < p_i^{II} < 2\pi$, the right-hand side of (12) is negative, so that this condition is fulfilled automatically. However, there are intervals of the parameter p_i^{II} where the right-hand side is positive, so that the condition (12) is not trivial.

The condition (12) can be resolved explicitly, using the above approximation (10):

$$v > \frac{\sin(\sqrt{2 + a^2 / \alpha v})}{a \sqrt{2 + a^2}}. \quad (13)$$

As an illustration, we can also consider the limit of a large spacing, $(a/2)^2 \gg 1$, although this case is far from the experimentally relevant region. In this limit, *without* employing the above approximation (10), Eq. (9) simplifies to $p_i^{II} \approx 1/v$, and the condition (12) takes the explicit form

$$a^2 > v^{-1} \sin v^{-1} - 4 \sin^2 \left(\frac{1}{2} v^{-1} \right). \quad (14)$$

Notice that Eqs. (13) and (14) concur at large a .

An implication of the above results is the existence of a critical velocity below which the oscillating tail is not possible. Because this prediction is quite interesting, we have checked it by direct simulations. Figure 4 shows evolution of the kink's shape at $a = 1$ and $\alpha = 0.1$ with the change of the kink's velocity (the kink is represented by the instantaneous voltage vs. time, as measured at an arbitrary chosen individual junction which we took at $n = 25$). It is clearly seen that the transition between the tailed and tailless fluxons *does* occur at some value of v between 0.173 and 0.143, corresponding to the panels (c) and (b) in Fig. 4. One still sees some small-amplitude *symmetric* tails at the small velocities 0.143 and 0.071 in the panels (b) and (a). By looking at these cases in a greater detail (not shown here), we conclude that

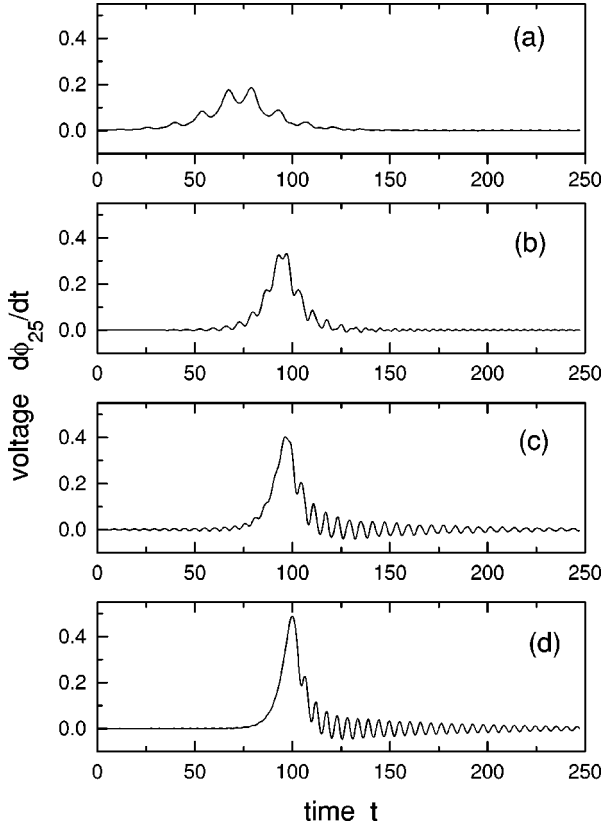


FIG. 4. The detailed structure of the numerically found voltage evolution for the passing fluxon in the one-dimensional annular Josephson junction array with the spacing $a = 1$, length $L = 50$, and dissipative constant $\alpha = 0.1$ at different values of the driving dc bias current corresponding to the following values of the steady fluxon velocity: (a) 0.071; (b) 0.143; (c) 0.173; (d) 0.257.

the small symmetric tails represent radiation which is emitted by the kink. The emitted waves have the phase velocities different from the kink's velocity, so that they *separate* from the kink. On the contrary to this, the one-sided tail seen in the panels (d) and (c) is rigidly attached to the kink's body, moving along with it.

The value of v at which the tail is expected to disappear for vanishingly small α according to Eqs. (8) and (12) can be easily found to be 0.244 [the simplified approximation (10) yields a close value 0.257]. As one sees, the predicted critical value of v turns out to be essentially larger than that revealed by the direct simulations. The reason for this discrepancy can be easily understood: according to Eq. (11), at the predicted critical point, the parameter $p_r^{\prime\prime}$ changes its sign not vanishing, but, on the contrary, diverging (i.e., going through infinity rather than through zero). On the other hand, the derivation of Eq. (11) assumed linearization with respect to the small $p_r^{\prime\prime}$. Thus, the above-mentioned critical velocity predicted by Eqs. (8) and (12) will be correct if it is very small. For finite v , one can easily estimate that an error in the predicted value may be $\sim \alpha$, which naturally explains the discrepancy observed at $\alpha = 0.1$. For still smaller α , numerical verification implies large computational times.

Lastly, Eqs. (8) and (12), as well as the simplified approximation (10), imply existence of an infinite set of smaller critical velocities, so that, for extremely small values of the dissipative constant, one would have an alternating

system of intervals of existence of the tailed and tailless kinks. We were not able to confirm this prediction numerically. The troubles are that even $\alpha = 0.1$ is probably too large for existence of this fine structure, and also that the tails reappearing at smaller v may have the tail with a midget amplitude.

IV. ANALYTICAL CONSIDERATION OF THE BUNCHED STATES

Now, let us consider two kinks moving at a distance m (measured in units of the array spacing) from each other. The kink in the forward position is overlapping with the front tail of the backward kink, and the latter one is overlapping with the trailing tail of the forward kink. The overlapping gives rise to two interaction forces between the kinks:¹³ the repulsive force generated by the exponentially decaying tail

$$F_{\text{rep}} = F_1 \exp(-p_r^I m), \quad (15)$$

and the sign-changing force generated by the decaying oscillating tail:

$$F_{\text{pin}} = F_2 \exp(p_r^{\prime\prime} m) \sin(p_i^{\prime\prime} m + \delta), \quad (16)$$

where δ is some phase-shift constant, and we assume that, by definition, $m > 0$. The latter force is actually a pinning one, amenable for existence of the bunched states of the kinks. The constants F_1 and F_2 in these expressions, as well as δ , are determined by matching the tails to the bodies of the moving kinks, and there is no way to find them analytically. Nevertheless, it will be demonstrated below that some essential results concerning the bunched states and transitions between them can be obtained, for small velocities, without knowing these constants.

As well as in the continuum model, in the discrete one a bunched state exists if the repulsive and pinning forces are in balance, $F_{\text{rep}} = F_{\text{pin}}$.¹³ A transition between different bunched states happens when F_{pin} attains its maximum corresponding to $|\sin(p_i^{\prime\prime} m + \delta)| = 1$ in Eq. (16), i.e., when

$$F_2 = F_1 \exp[(-p_r^I + p_r^{\prime\prime})m]. \quad (17)$$

A quantity of special interest is the number of oscillations of the small-amplitude field trapped between the two kinks (this field is nothing else but the trailing tail of the forward kink). According to Eqs. (17) and (3), at the moment of the jump between different bunched states this number is

$$\Delta n = \frac{m p_i^{\prime\prime}}{2\pi} = \frac{p_i^{\prime\prime}}{2\pi(p_r^I - p_r^{\prime\prime})} \ln \frac{F_1}{F_2}, \quad (18)$$

where the phase constant δ is neglected.

Our objective will be to compare the analytical prediction (18) with numerical results, as the moment of the jump between different states can be easily identified by looking at *IVC* (Fig. 3). However, the comparison is hampered by absence of the information about the constant F_2/F_1 , as well as by the neglect of the constant δ in Eq. (18). All these problems compel us to confine the comparison to the range of small velocities. Indeed, the above analysis clearly suggests that not only the unknown constants F_2/F_1 and δ , but also the known ones p_r^I and $p_r^{\prime\prime}$ have no singularities at v

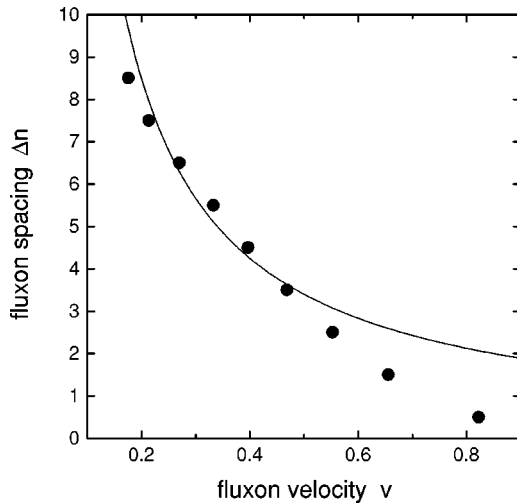


FIG. 5. Comparison of the analytical approximation with direct numerical simulations for $L=100$ and $a=1.0$. Circles show the numerically found threshold velocities at which switching between consecutive fluxon bunched states occur with decrease of the bias current from $\gamma=0.5$ down to $\gamma=0$. The solid line shows the hyperbola (19).

$\rightarrow 0$, hence they can be assumed approximately constant at small v . On the other hand, the parameter p_i^{II} is diverging at $v \rightarrow 0$ [see Eq. (10)], that is why the asymptotic form of the expression (18) becomes very simple form in this limit,

$$\Delta n \approx C/v, \quad (19)$$

with an unknown constant C .

For comparison with this, we solved numerically Eqs. (7) and (8) for given v and the discreteness parameter (lattice spacing) a . Figure 5 shows the comparison of the hyperbola (19) with numerical simulations for $L=100$ and $a=1.0$. Circles show the threshold velocities, at which the switching between consecutive fluxon bunched states occurs when decreasing the bias current from $\gamma=0.5$ down to much smaller γ , as found from direct numerical simulations. We defined the number of the trapped oscillations Δn corresponding to this switching point as the actual number of the oscillations between the two kinks at this point plus $\frac{1}{2}$.

The solid curve in Fig. 5 is the hyperbola (19) with the unknown constant fitted to the numerical data at small v . One can see that, in this range, our simple analytical model qualitatively agrees with the simulations. There is a large discrepancy at $v > 0.5$, where, however, it is very hard to develop a consistent analytical approach.

V. DISCUSSION

In the previous section we have evaluated the velocities at which the switching between different bunched states takes place. Still, the question of the velocity dependence on the driving bias current for various states was left open. The difference between the equilibrium velocities for the numerically simulated single-fluxon and bifluxon cases is summarized in Fig. 6. The simulation where performed for $L=100$, $a=1.0$, and $\alpha=0.3$. The corresponding single-fluxon velocity v_{1F} and the bifluxon velocity v_{2F} have been taken at the same values of the bias current. The arrows show the

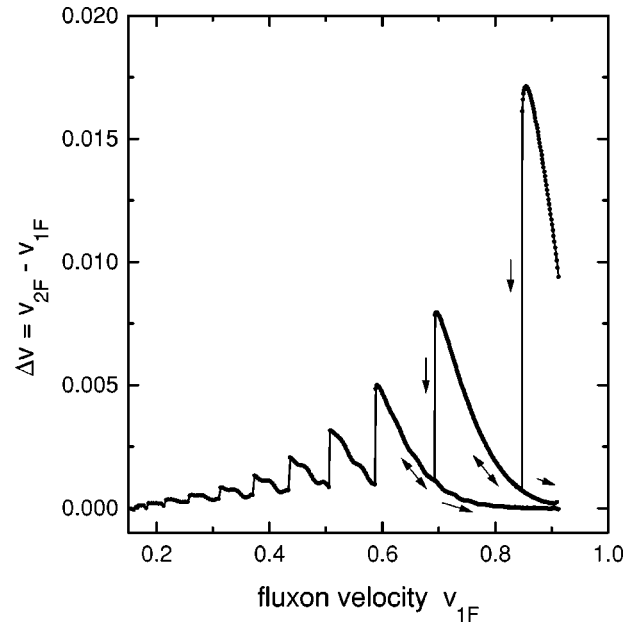


FIG. 6. The difference between the steady-state velocities for the numerically found single-fluxon and bifluxon states for $L=100$, $a=1.0$, and $\alpha=0.3$.

hysteresis for different directions of variation of the bias current. The simulations reveal that the largest difference between the single-fluxon and bifluxon velocities is attained at the switching points between the different branches. In general, two bound fluxons “help” each other to reduce the dissipative losses and therefore their velocity is higher than that of the single fluxon.

All the predictions obtained in this work in terms of the current-voltage characteristic of the one-dimensional arrays of the pointlike Josephson junctions should be amenable to a straightforward experimental check. Note that the above analysis did not take into regard fluctuations. In principle, fluctuations can destroy bound states of solitons (while an individual fluxon is a very robust object even in the presence of strong fluctuations). However, at least some of the bound states predicted in this work are fairly robust too (e.g., those shown in Fig. 2). The intensity of the thermal fluctuations in experiment can be suppressed by cooling down the sample, while the quantum fluctuations are usually extremely weak for the fluxons, that are, effectively, heavy semiclassical quasiparticles. Therefore, the fluctuations should not be a serious problem in the present context.

It is relevant to mention that other steps on IVC of the one-dimensional discrete Josephson array, predicted theoretically in Ref. 1 and observed experimentally in Ref. 2, are produced by the resonant interaction between a 2π -kink and quasilinear lattice modes (also called “plasma waves” or “phonons”). In the experiment, the multifluxon steps predicted here can be easily distinguished from the fluxon-phonon ones, because the location and size of the two types of the steps are drastically different. Comparison of the absolute values of the voltage should allow one to determine the actual number of the 2π -kinks in the bunched state that gives rise to the steps. The experimental signature of fluxon bunching is that the voltages of fluxon-phonon resonant steps on the current-voltage characteristics should not scale ex-

actly proportional to the number of fluxons in the array. The voltage of multifluxon resonances is expected to be high than that of the single-fluxon resonance multiplied by the number of fluxons. Another natural question is how to excite a desired number of bunched fluxons in the dynamic state. A way to do this can be by using a strong localized perturbation, generated, e.g., by a current pulse through one of the point-like junctions of the array.

It is interesting to note that attractively interacting SG kinks similar to those forming the $(2\pi + 2\pi)$ -kink bunched states studied here were considered long time ago by Nakajima and co-workers.¹⁵ The authors of that work simulated a perturbed continuum SG system, using a *discrete* numerical scheme similar to Eq. (1). The bound states found in Ref. 15 were not attributed to the discreteness of the system. As it was mentioned above, the bunched states of the kinks with the same polarity do not exist in the continuum SG model, unless the surface losses are added to it. Therefore, we conjecture that the bunched states reported in Ref. 15 were actually produced by the discreteness of the numerical scheme.

Finally, we would like to point out that fluxon dynamics and the mechanism of interactions between the fluxons discussed in the present paper appear to be relevant for more complex systems, such as two-dimensional Josephson junction arrays. Since the dynamics of those structures is rather complicated, it is natural to split the problem into parts and study first the interaction between fluxons moving in two neighboring rows. First experimental results using two

coupled DJTLs have recently been reported.^{16,17} In this case, one is dealing with the interaction between inductively coupled DJTLs. Using the approach developed in the model of the stacked Josephson junctions,¹⁸ its generalization for some of the two-dimensional Josephson junction arrays has been recently proposed.¹⁹ Due to the interaction between individual DJTLs in the array, the solitons moving in different lines may form new coherent structures that propagate along the system. For example, with regard to the bunched fluxon states discussed in this paper, we can predict that more complex bunched states should exist between fluxons simultaneously moving in neighboring rows of the array. In such a case, the small-amplitude waves induced by the moving fluxon in one row may couple to adjacent lines and induce an effective interaction potential for the fluxons moving in these rows. In this case the experimentally observable consequences of fluxon bunching are expected to be similar to that discussed in present paper. The major difference to expect is that the voltage will be smaller proportionally to the coupling between adjacent junction rows.

ACKNOWLEDGMENTS

A.V.U. is grateful to the members of the Electron Devices Section of ETL (Tsukuba, Japan) for their hospitality during his stay at ETL and also to the AIST for financial support. This work was partly supported by a Grant G0464-247.07/95 from the Germany-Israel Foundation.

-
- ¹A. V. Ustinov, M. Cirillo, and B. A. Malomed, *Phys. Rev. B* **47**, 8357 (1993).
- ²H. S. J. van der Zant, T. P. Orlando, S. Watanabe, and S. H. Strogatz, *Phys. Rev. Lett.* **74**, 174 (1995).
- ³M. Cirillo, R. D. Parmentier, and B. Savo, *Physica D* **3**, 565 (1981).
- ⁴K. Nakajima, Y. Onodera, T. Makamura, and R. Sato, *J. Appl. Phys.* **45**, 4095 (1974).
- ⁵H. S. J. van der Zant, D. Berman, T. P. Orlando, and K. A. Delin, *Phys. Rev. B* **49**, 12 945 (1994).
- ⁶A. V. Ustinov, M. Cirillo, B. H. Larsen, V. A. Oboznov, P. Carelli, and G. Rotoli, *Phys. Rev. B* **51**, 3081 (1995).
- ⁷P. Caputo, A. V. Ustinov, N. Iosad, and H. Kohlstedt, *J. Low Temp. Phys.* **106**, 353 (1997).
- ⁸S. Watanabe, S. H. Strogatz, H. S. J. van der Zant, and T. P. Orlando, *Phys. Rev. Lett.* **74**, 379 (1995).
- ⁹M. Peyrard and M. D. Kruskal, *Physica D* **14**, 88 (1984).
- ¹⁰W. J. Johnson, Ph.D. Thesis, University of Wisconsin, 1968 (unpublished).
- ¹¹A. Davidson, N. F. Pedersen, and S. Pagano, *Appl. Phys. Lett.* **48**, 1306 (1986).
- ¹²B. Dueholm, O. A. Levring, J. Mygind, N. F. Pedersen, O. H. Sørensen, and M. Cirillo, *Phys. Rev. Lett.* **46**, 1299 (1981).
- ¹³B. A. Malomed, *Phys. Rev. B* **47**, 1111 (1993).
- ¹⁴R. D. Bock, J. R. Phillips, H. S. J. van der Zant, and T. P. Orlando, *Phys. Rev. B* **49**, 10 009 (1994).
- ¹⁵K. Nakajima, Y. Sawada, and Y. Onodera, *J. Appl. Phys.* **46**, 5272 (1975).
- ¹⁶A. E. Duwel, H. S. J. van der Zant, and T. P. Orlando, *IEEE Trans. Appl. Supercond.* **5**, 3357 (1995).
- ¹⁷P. Caputo, H. Kohlstedt, A. V. Ustinov, I. V. Vernik, and V. A. Oboznov, in *Proceedings of the 5th International Superconductive Electronics Conference*, Nagoya, Japan, 1995, pp. 447–449.
- ¹⁸S. Sakai, P. Bodin, and N. F. Pedersen, *J. Appl. Phys.* **73**, 2411 (1993).
- ¹⁹A. Petraglia, N. F. Pedersen, P. L. Christiansen, and A. V. Ustinov, *Phys. Rev. B* **55**, 8490 (1997).